Cell Reports
Article

Open ACCESS

Regulation of the Apolipoprotein Gene Cluster by a Long Noncoding RNA

Paul Halley,[1,2,5] Beena M. Kadakkuzha,[1,2,5] Mohammad Ali Faghihi,[1,2] Marco Magistri,[1,2] Zane Zeier,[1,2] Olga Khorkova,[3] Carlos Coito,[3] Jane Hsiao,[3] Matthew Lawrence,[4] and Claes Wahlestedt[1,2,*]

[1]Center for Therapeutic Innovation, University of Miami, Miller School of Medicine, NW 10th Avenue, Miami, FL 33136, USA
[2]Department of Psychiatry and Behavioral Sciences, Miller School of Medicine, University of Miami, NW 10th Avenue, Miami, FL 33136, USA
[3]OPKO-CURNA, 10320 USA Today Way, Miramar, FL 33025, USA
[4]RxGen, Inc., 100 Deepwood Drive, Hamden, CT 06517, USA
[5]These authors contributed equally to this work
*Correspondence: cwahlestedt@med.miami.edu

http://dx.doi.org/10.1016/j.celrep.2013.12.015

SUMMARY

Apolipoprotein A1 (APOA1) is the major protein component of high-density lipoprotein (HDL) in plasma. We have identified an endogenously expressed long noncoding natural antisense transcript, *APOA1-AS*, which acts as a negative transcriptional regulator of APOA1 both in vitro and in vivo. Inhibition of *APOA1-AS* in cultured cells resulted in the increased expression of APOA1 and two neighboring genes in the *APO* cluster. Chromatin immunoprecipitation (ChIP) analyses of a ~50 kb chromatin region flanking the *APOA1* gene demonstrated that *APOA1-AS* can modulate distinct histone methylation patterns that mark active and/or inactive gene expression through the recruitment of histone-modifying enzymes. Targeting *APOA1-AS* with short antisense oligonucleotides also enhanced *APOA1* expression in both human and monkey liver cells and induced an increase in hepatic RNA and protein expression in African green monkeys. Furthermore, the results presented here highlight the significant local modulatory effects of long noncoding antisense RNAs and demonstrate the therapeutic potential of manipulating the expression of these transcripts both in vitro and in vivo.

INTRODUCTION

In recent years, long noncoding RNAs (lncRNAs) have been shown to play important functional roles as regulators of gene expression (Ansari, 2009; Faghihi et al., 2010; Huarte et al., 2010; Katayama et al., 2005; Martinho et al., 2004; Modarresi et al., 2012), through the recruitment of the complex epigenetic machinery that dictates distinctive chromatin signatures involved in active transcription (Kaikkonen et al., 2011; Magistri et al., 2012; Rinn et al., 2007; Tsai et al., 2010; Wang et al., 2011b). One such group of lncRNAs is the natural antisense transcripts (NATs), which are transcribed from the opposite DNA strand to their specific partner protein-coding (or noncoding) genes. The most common example of antisense transcription is the pairing of a NAT with an overlapping protein-coding (sense) transcript, whereby NAT expression can lead to an increase (concordant) or decrease (discordant) in sense expression (Faghihi and Wahlestedt, 2009). Modulatory effects of antisense ncRNAs on neighboring genes have also been reported in yeast (Camblong et al., 2007) and mammalian imprinting (Nagano et al., 2008; Sleutels et al., 2002), suggesting that the regulatory role of NATs can extend beyond their sense partners to the overlapping chromatin region.

The observation that more than 70% of mammalian transcriptional units show evidence of antisense transcription not only indicates the biological importance of NATs but could also have various therapeutic implications (Katayama et al., 2005; Lehner et al., 2002; Wahlestedt, 2006). For example, identifying and inactivating a discordantly acting NAT, using various RNAi approaches, could lead to derepression and subsequent "switching on" of a gene of interest (Wahlestedt, 2006). Very recently, our group has successfully used this approach to substantially increase the expression of the therapeutic target brain-derived neurotrophic factor (BDNF), through inhibition of endogenous noncoding antisense transcripts that repress *BDNF* transcription (Modarresi et al., 2012). We have now identified a NAT for another therapeutically relevant gene, the Apolipoprotein A1 (*APOA1*).

APOA1 is the major protein component of high-density lipoprotein (HDL) in plasma (Barbaras et al., 1987) and is synthesized primarily in the liver (80%) and small intestine (10%) (Elshourbagy et al., 1985). It plays a key role in reverse cholesterol transport, promoting cholesterol efflux from tissues by acting as a cofactor for the lecithin cholesterol acyltransferase (Glomset, 1968). A low HDL cholesterol concentration reflects increased susceptibility to atherosclerosis and raising HDL pharmacologically remains a proposed strategy to reduce the occurrence of cardiovascular diseases (Green et al., 1979;Livshits et al., 1997; Rader, 2002). The genes encoding human *APOA1*, as well as apolipoproteins *C3*, *A4*, and *A5*, are clustered on chromosome 11q23.3 (Figure 1A), with *APOA1*, *APOA4*, and *APOA5* transcribed 5′ to 3′, and *APOC3* transcribed in the opposite direction

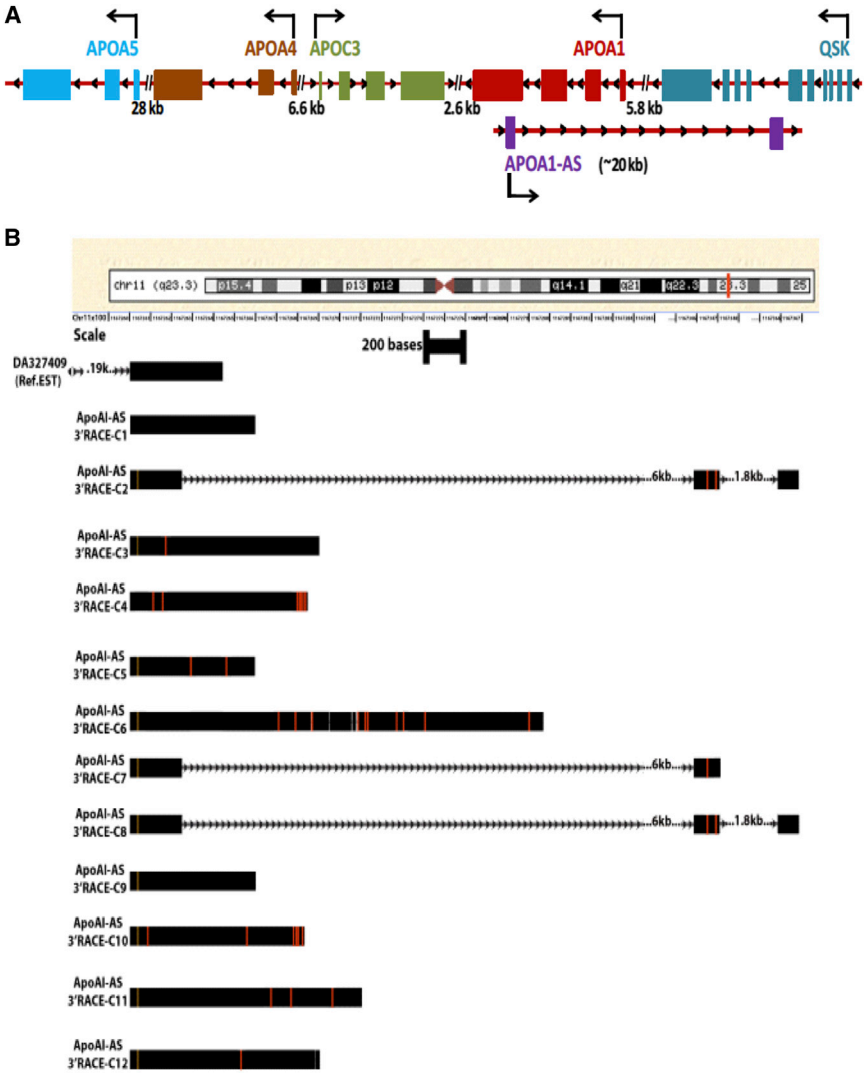

Figure 1. *APO* Gene Cluster and *APOA1-AS* NAT Organization on Human Chromosome 11

The direction of transcription is indicated by arrows.

(A) The antisense transcript *APOA1-AS* (EST DA327409) has two exons; the first exon is partially overlapping with the forth exon of *APOA1*, and the second exon is overlapping with the intronic region of *QSK* gene.

(B) The splice variants obtained from 3′ and 5′ RACE using primers based on the DA327409 sequence.

(Antonarakis et al., 1988). Although previous studies have shown that transcription at the human apolipoprotein gene cluster (*A1/C3/A4/A5*) is dependent on specific chromatin structures, such as the CTCF/cohesion chromatin insulators (Mishiro et al., 2009), relatively little is known about the epigenetic factors influencing *APOA1* expression. Here, we report a NAT-mediated mechanism of *APOA1* transcriptional regulation that involves the recruitment of multiple chromatin-modifying complexes to the *APO* gene cluster. We demonstrate that targeting this NAT, using both small interfering RNAs (siRNAs) and antisense oligonucleotides (ASOs), can induce an increase in *APOA1* expression both in vitro and in vivo, respectively.

RESULTS

Characterizing an Overlapping Antisense Transcript at the *APO* Gene Cluster

APOA1 mRNA is transcribed from the negative strand of chromosome 11 and contains four exons. A potential *APOA1*-natural antisense EST (EST sequence DA327409) was identified, using UCSC genome browser (http://genome.ucsc.edu) (Figure S1), that is transcribed from the positive strand of the *APOA1* locus and has two exons, positioned ~20 kb apart (Figure 1A). This *APOA1* antisense transcript (*APOA1-AS*) shares a 123-nucleotide-long region overlapping with the fourth exon of *APOA1* mRNA (Figure 1A). In order to find the complete sequence (e.g., transcription start site [TSS]), alternative splicing, and 3′ end of APOA1-AS transcript, RACE (rapid amplification of the 3′ or 5′ cDNA ends), experiments were performed with primers designed based on the EST sequence. RACE expanded the EST sequence from both 3′ and 5′ ends and determined splice variants with additional 3′ exons (Figure 1B). We next examined a panel of RNAs from human tissues for the presence of *APOA1* and *APOA1-AS* transcripts by quantitative RT-PCR, using specifically designed probes. Both *APOA1* and *APOA1-AS* transcripts were expressed in all tissues examined; however, there were significant differences in their expression levels (Figure 2A). *APOA1* mRNA was highest in the liver, an order of magnitude less in small intestine, and two orders of magnitude less in colon. *APOA1-AS* was highly expressed in ovary, cervix, testis, and thyroid. The ratio of *APOA1/APOA1-AS* was also seen to vary for many of the tissues examined (Figure 2B). Liver, small intestine, and colon showed 10^3-fold higher expression levels of *APOA1* mRNA compared to *APOA1-AS*, whereas testis, heart, and 12-week embryo showed a 10^2-fold difference. The *APOA1/APOA1-AS* ratios were one or less than 10-fold in thymus, ovary, spleen, kidney, esophagus, thyroid, adipose tissue, skeletal muscle, placenta, lung, prostate, trachea, and brain.

APOA1-AS Transcript Acts as a "Temporal Switch" to Regulate *APOA1* Expression

The liver expresses large amounts of APOA1, accounting for more than 70% of circulating APOA1 protein in the blood

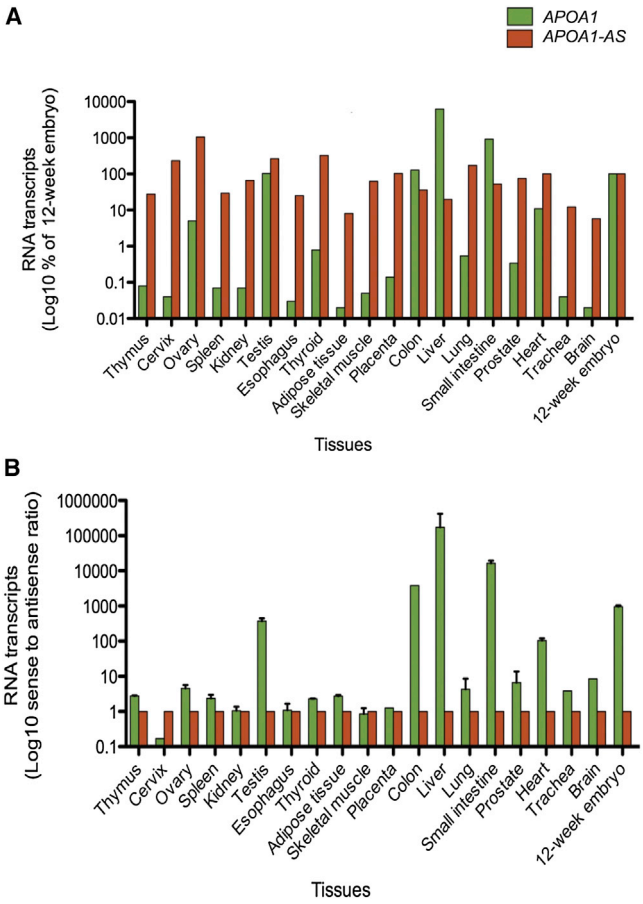

Figure 2. Characterization of the Expression Profiles of *APOA1* and *APOA1-AS*

(A) Quantitative RT-PCR analysis of *APOA1* and *APOA1-AS* in RNA samples from a panel of different human tissues; each transcript was normalized to the value of the same transcript in 12-week embryo.

(B) The ratio of *APOA1*-to-*APOA1-AS* transcripts was measured in commercial RNAs obtained from various tissues. Graphs represent mean relative expression values ± SEM.

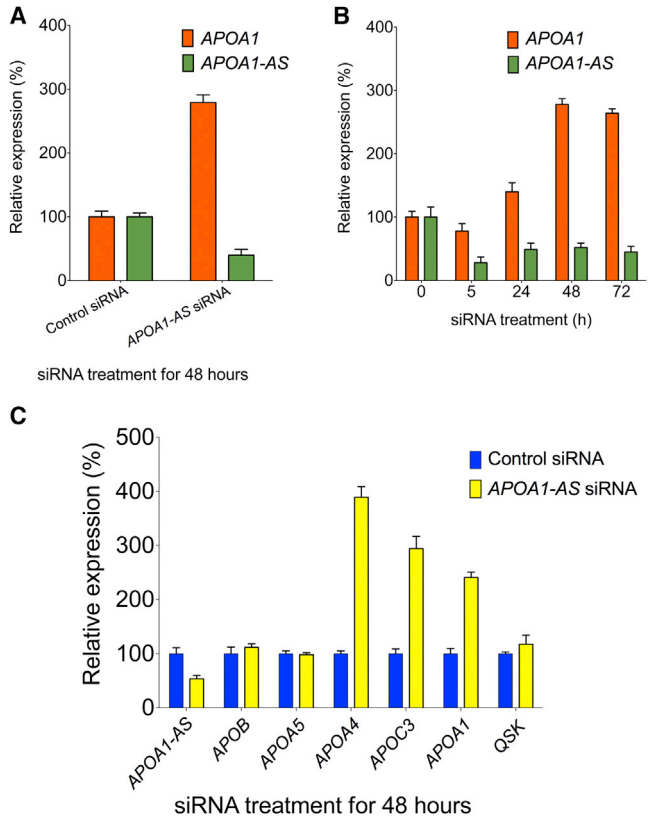

Figure 3. siRNA-Mediated Downregulation of *APOA1-AS*

(A) HepG2 cells were transfected with *APOA1-AS* siRNA and control siRNA for 48 hr, and the levels of *APOA1* and *APOA1-AS* genes were measured with quantitative RT-PCR. See also Figures S1, S2, and S3.

(B) HepG2 cells were transfected with *APOA1-AS* siRNA, total RNA was collected after 5, 24, 48, and 72 hr, and the transcript levels of *APOA1* and *APOA1-AS* were measured with quantitative RT-PCR.

(C) HepG2 cells were transfected with *APOA1-AS* siRNA and control siRNA for 48 hr. Quantitative RT-PCR was used to measure the expression of the genes belonging to the *APO* gene cluster. Graphs represent mean relative expression values ± SEM.

See also Figure S2.

(Eisenberg, 1984). In order to identify any direct link between the sense-antisense expression levels of *APOA1* and *APOA1-AS* transcripts, we next treated liver HepG2 cells with specific siRNAs designed against *APOA1-AS*. The sequences of all three siRNAs and the areas of the *APOA1-AS* transcript targeted by each are presented in Figure S1. Although all three siRNAs tested showed significant knockdown of *APOA1-AS* (Figure S2), siRNA 1 showed the highest efficiency (~65%), leading to ~3-fold upregulation of the *APOA1* transcript (Figures 3A and S3) and was thus used in all subsequent experiments. A time course experiment was performed, whereby total RNA was extracted at 5, 12, 24, 48, and 72 hr after transient transfection with the *APOA1-AS* siRNA. *APOA1-AS* transcript levels were significantly reduced after 5 hr (up to 90%) (Figure 3B) and returned to ~60% compared to negative control siRNA treatment after 24 hr. *APOA1* mRNA concentration was increased over the time course from 12 hr and reached plateau at 72 hr (Figure 3B).

The upregulation pattern of *APOA1* mRNA over 72 hr indicates that transient reduction of *APOA1-AS* expression is sufficient for initiating the transcriptional upregulation of *APOA1* gene, achieving 3-fold elevation at 48 and 72 hr. These results indicate a functional role of endogenous *APOA1-AS*, whereby it can act analogous to a molecular switch to dictate the expression levels of the *APOA1* sense gene.

APOA1-AS Modulates Multiple Genes in the *APO* Gene Cluster

We hypothesized that *APOA1-AS* may modulate transcriptional regulation not only of *APOA1* but also other members of the *APO* gene cluster (*C3/A4/A5*) located in close proximity on the chromatin. Quantitative PCR (qPCR) analysis of *APOA1/APOC3/APOA4/APOA5* transcripts in HepG2 cells transfected with the *APOA1-AS* siRNA showed that *APOC3* and *APOA4* were upregulated ~3- and ~4-fold, respectively, but *APOA5*

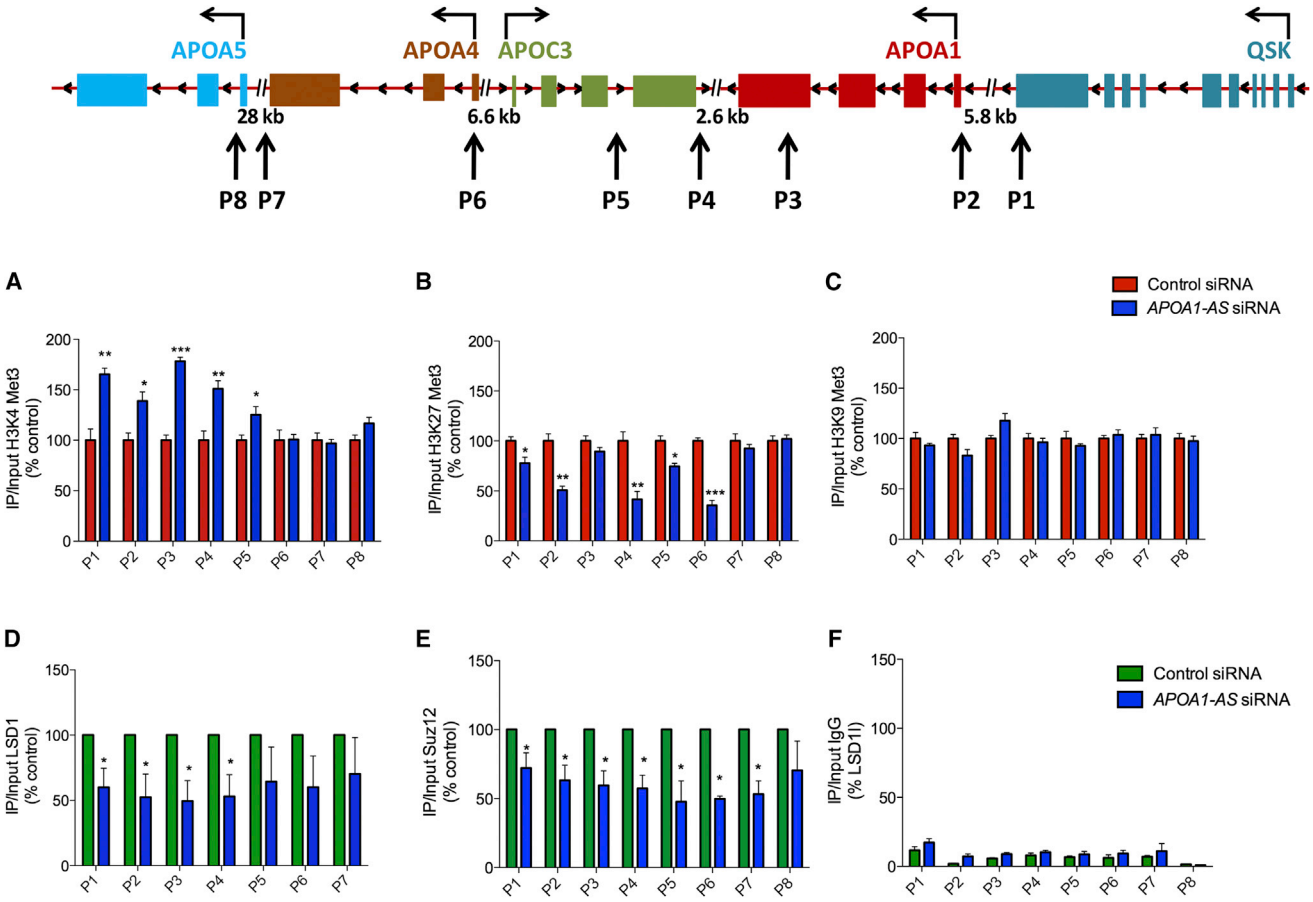

Figure 4. ChIP Analysis for Histone Modifications on the 50 kb Chromatin Region of *APO* Gene Cluster

Upper panel: Schematic representation of the ChIP Ps covering ~50 kb chromatin region of *APO* gene locus. See also Table S1.

Lower panel: HepG2 cells were transfected with *APOA1-AS* siRNA and control siRNA for 48 hr.

(A–E) Cells were lysed, and chromatin was collected for ChIP analysis of (A) H3K4-met3, (B) H3K27-met3, (C) H3K9 met3, (D) LSD1, and (E) SUZ12 levels along the ~50 kb chromatin region. IP, immunoprecipitated.

(F) Background ChIP observed with a control IgG antibody (n = 3).

Graphs represent mean values ± SEM. *p < 0.05, **p < 0.01, and ***p < 0.001, two-tailed Student's t test. See also Table S1.

mRNA concentration was unchanged (Figure 3C). To further test the extent of *APOA1-AS*-mediated transcriptional regulation, we measured the expression of the neighboring inosine-guanosine kinase (*QSK*), a serine kinase located 6 kb upstream of *APOA1* gene, which has intronic overlap with the second exon of *APOA1-AS* (Figure 1A). Interestingly, *QSK* concentration was not affected by the *APOA1-AS* knockdown, indicating a degree of locus specificity and a possible chromatin boundary region relating to *APOA1-AS* activity. To evaluate the *trans*-acting properties of the *APOA1-AS*, Apolipoprotein B (*APOB*), another member of the *APO* gene family that is transcribed from chromosome 22 and is also involved in cholesterol pathway, was also examined (Figure 3C). We did not observe any change in *APOB* mRNA concentration after knockdown of *APOA1-AS*, suggesting that this regulation of the *APO* gene cluster by *APOA1-AS* occurs locally (i.e., in *cis*). Together, these findings highlight the significant role played by a *cis*-acting NAT in local chromatin regulation.

The *APO* Gene Cluster Is Epigenetically Regulated by *APOA1-AS*

We next hypothesized that *APOA1-AS* could function as a mediator of suppressive epigenetic markers, through the recruitment of chromatin-modifying complexes. To examine *APOA1-AS*-associated chromatin modifications at the *APO* gene cluster, we performed chromatin immunoprecipitation (ChIP) experiments to measure the levels of trimethylated lysines 4, 9, and 27 on histone H3 following siRNA-mediated *APOA1-AS* knockdown. H3K4-met3 marks transcriptionally active chromatin, whereas, H3K9-met3 and H3K27-met3 are considered to be repressive chromatin marks (Kouzarides, 2002; Strahl and Allis, 2000). Eight primer sets (Ps) were designed to span a 50 kb region encompassing *APOA1*, *APOC3*, *APOA4*, and *APOA5* (Figure 4A; Table S1).

ChIP, followed by qPCR analysis, showed distinctive changes in H3K4-met3 and H3K27-met3 levels, whereas no significant changes were observed in H3K9-met3. The amplicons amplified

by P1–P5 demonstrated significantly elevated levels of the active marker H3K4-met 3 in HepG2 cells treated with the *APOA1-AS* siRNA (Figure 4A). In addition, levels of the repressive mark H3K27-met3 for the P1–P6 region, which also included the promoters for *APOC3* and *APOA4*, were significantly reduced (Figure 4C), whereas H3K9-met3, another mark associated with gene silencing, was unchanged (Figure 4D). These amplicons spanned the promoter of *APOA1*, as well as a specific enhancer element involved in the regulation of *APOA1*/*APOC3*/*APOA4*, thus indicating increased transcriptional activity. It is interesting to note that P6, which represented the amplicon at the promoter of *APOA4*, demonstrated no change in H3K4 trimethylation (Figure 4B) but a rather pronounced reduction in the levels of repressive chromatin marker H3K27-met3 (Figure 4C).

It has previously been shown that ncRNAs act as scaffold for the locus-specific recruitment of functionally related chromatin-modifying enzymes (Guttman et al., 2011; Tsai et al., 2010). In order to explain the observed changes in histone modifications, further ChIP experiments were performed using antibodies for (1) the lysine (K)-specific demethylase 1 (LSD1), a nuclear protein that is known to induce gene silencing through the removal of active methyl marks, primarily from H3K4 (Shi et al., 2004), and (2) the Suppressor of Zeste 12 homolog (SUZ12), a key component of the polycomb recessive complex 2 (PRC2), which has been shown to mediate chromatin silencing through H3K27 trimethylation (Cao et al., 2002; Kuzmichev et al., 2002). In addition to the increase in active H3K4me3 at the *APOA1* promoter (P1–P5) following siRNA treatment, these amplicons (P1–P4) also exhibited significantly reduced LSD1 occupancy (Figure 4E), indicating that *APOA1-AS*, at least in part, induces the transcriptional silencing of the *APOA1* gene through LSD1 recruitment. Furthermore, the decrease in repressive H3K27me3 marks on the amplicons for P1–P6 following siRNA treatment also coincided with a marked reduction of SUZ12 occupancy for this region, suggesting that the observed increase in *APOA4* and *APOC3* gene expression is due to a disruption of *APOA1-AS*-mediated PRC2 interaction. ChIP experiments were also carried out for the same samples using an IgG control antibody, to confirm that all chromatin immunoprecipitated was specific to LSD1 or SUZ12 and could not be attributed to background, nonspecific binding (Figure 4F).

ASOs Targeting *APOA1-AS* Induce *APOA1* Upregulation In Vitro and In Vivo

Given the clear therapeutic potential for the treatment of atherosclerosis, we further tested our hypothesis by examining whether targeting *APOA1-AS* could promote hepatic *APOA1* expression in vivo. Over 80 phosphorothioate-backbone ASOs were designed to cover the full *APOA1-AS* sequence. To test their potency to upregulate *APOA1* transcript levels, these oligonucleotides (termed AntagoNATs) were first tested in HepG2 cells. Forty-eight hours after transfection, total RNA was isolated from these cells, and *APOA1* mRNA concentration was measured by quantitative RT-PCR. A number of AntagoNATs induced a significant increase of *APOA1* mRNA expression (Figure S4). These active AntagoNATs appeared to cluster into two major "hot spots" on the *APOA1-AS* sequence. To confirm the existence of the hot spots, we then chose two regions for a more detailed survey in single nucleotide steps: one around a hot spot (CUR-0461 to CUR-0284), the other around a mostly inactive area (CUR-0279 to CUR-0473). AntagoNATs designed around the hot spot produced on average a 1.7-fold upregulation of *APOA1* mRNA, whereas oligonucleotides designed around an inactive area produced an upregulation of 1.05-fold on average, which supported the hot spot hypothesis (Figure S4). We then mapped active oligonucleotides to the secondary structure of *APOA1-AS* (Figure S4). Active AntagoNATs were associated almost exclusively with one arm of the molecule. The two "hot spots," which are separated by about 200 bases in the linear NAT sequence, mapped close to each other in the secondary structure and were associated with a system of stable hairpin loops. These results indicate that differences in AntagoNAT activity may be due to their interactions with secondary and consequently tertiary structure of NATs. Finally, AntagoNATs invoking the largest upregulation were selected and chemically modified to increase their stability. They were then tested in vitro, in both human (HepG2) and African green monkey cells, to identify the combination of sequence and chemical modifications that produced the highest upregulation of *APOA1* in both species. For this transition between human and monkey cells, the AntagoNATs were specifically designed based on regions for which the human and rhesus genome sequences were identical. Figure 5 demonstrates the increase in *APOA1* expression observed in HepG2 cells following treatment with two such AntagoNATs, the most active of which (CUR-1906) induced a 2- to 4-fold upregulation of *APOA1* mRNA and protein levels (see also Figure S5). Figure 6A demonstrates *APOA1* mRNA expression in primary monkey hepatocytes treated with active AntagoNATs relative to a same-chemistry control oligonucleotide (dashed line). The sequences and modifications of these AntagoNATs, as well as the regions targeted by each, are presented in Figure S6. The majority of the chemically modified AntagoNATs screened induced no cytotoxicity at concentrations up to 4000 nM, as determined by the MTS test. From this pool of active AntagoNATs, CUR-962, a 12-mer single-stranded oligonucleotide with phosphorothioate backbone and five LNA modifications in gapmer configuration (LLXXXXXXXLLL, where "L" indicates LNA), was selected and manufactured on a larger scale for in vivo testing.

African green monkeys (n = 4/group) received three 10 mg/kg intravenous injections of the AntagoNAT (CUR-962), or a chemically matched inactive control AntagoNAT (CUR-963), over a 5-day period (days 1, 3, and 5). The CUR-963 control had no effect on *APOA1* mRNA or protein expression compared to baseline values during in vitro testing. RT-PCR analyses of liver biopsies taken 3 months prior to injection and 72 hr after final injection revealed an increase in *APOA1* mRNA expression for all four monkeys that received the active AntagoNAT, CUR-962, compared to those receiving the control CUR-963. On average, liver biopsies from the AntagoNAT-treated cohort demonstrated a ~1.7-fold intraindividual increase of *APOA1* mRNA compared to pretreatment biopsy samples ($p = 0.04$; Figure 6B), whereas expression levels in the control CUR-963-treated group were unchanged. Furthermore, circulating APOA1 protein concentrations in the AntagoNAT-treated animals were elevated by ~10–15 mg/dl on days 6, 15, and 20

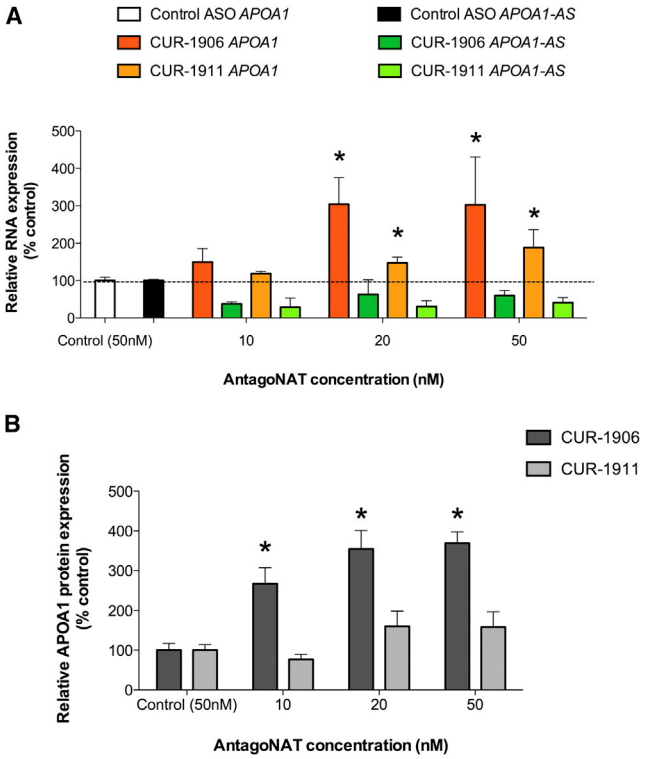

Figure 5. ASOs Targeting *APOA1-AS* Can Increase *APOA1* mRNA and Protein Expression In Vitro

HepG2 cells were transiently transfected with AntagoNATs against *APOA1-AS*. CUR-1906 induced a 2- to 4-fold upregulation of *APOA1* mRNA (A) and protein (B) levels ($3 < n < 6$; $^*p < 0.05$). Graphs represent mean relative expression values ± SEM. See also Figure S5.

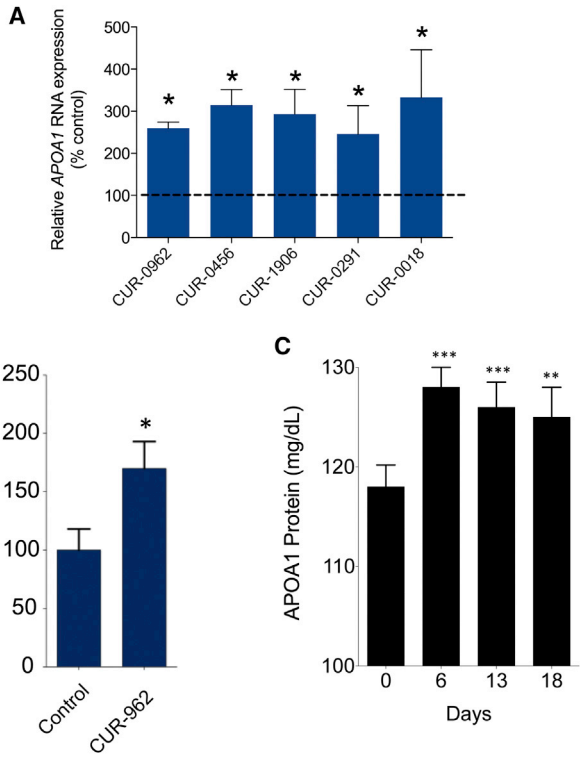

Figure 6. ASOs Targeting *APOA1-AS* Can Increase *APOA1* mRNA and Protein Expression In Vivo

(A) Primary African green monkey hepatocytes were transiently transfected with AntagoNATs against *APOA1-AS* and induced a 2- to 4-fold upregulation of *APOA1* mRNA.

(B) Liver biopsies of monkeys ($n = 4$) treated with CUR-962 showed ~1.7-fold increase in *APOA1* mRNA concentration compared to baseline biopsy samples ($p = 0.04$). All four active AntagoNAT-treated monkeys showed elevated liver *APOA1* mRNA concentration.

(C) Measurement of APOA1 protein in African green monkey blood ($n = 4$). We observed a significant increase in circulating APOA1 protein by an average of 10 mg/dl and up to 15 mg/dl.

All graphs represent mean values ± SEM. $^*p < 0.05$, $^{**}p < 0.01$, and $^{***}p < 0.001$. See also Figure S6.

postinjection, compared to their matched pretreatment biopsies ($p < 0.01$; Figure 6C).

DISCUSSION

Within the last decade, ncRNAs have come to represent an exciting avenue for the treatment of diseases (Calin and Croce, 2006; McDermott et al., 2011; Miller and Wahlestedt, 2010; Pastori and Wahlestedt, 2012; Taft et al., 2010; van Rooij and Olson, 2007). By identifying and characterizing regulatory antisense transcripts, it may be possible to manipulate the expression of a therapeutic gene for a range of indications. In this regard, siRNAs, which direct selective mRNA degradation using the multicomponent RNA-induced silencing complex (Zamore et al., 2000), offer a fast and robust approach to study RNA-mediated gene regulatory mechanisms in vitro. Alternatively, short ASOs can be specifically modified for increased stability, high specificity, and potency, and are a powerful tool to attain direct gene silencing in vivo (Dias and Stein, 2002; Veedu and Wengel, 2009). Here, we have identified a mechanism by which an endogenous, long noncoding antisense RNA can modulate the expression of *APOA1* and multiple neighboring genes, by facilitating the interaction of histone-modifying complexes with a specific target locus. ChIP analyses of H3K4, H3K9, and H3K27 trimethylation status following *APOA1-AS* knockdown demonstrated that the interplay between H3K27 methylation and H3K4 demethylation within the same chromatin region is critical to maintaining an active chromatin state for *APOA1*, *APOC3*, and *APOA4* expression.

LSD1 is known to remove methyl marks primarily from H3K4, which are associated with transcriptionally active promoters, and pharmacological LSD1 inhibitors have also been shown to enhance H3K4 methylation, leading to the derepression of epigenetically suppressed genes (Wang et al., 2011a). Although it has been reported that LSD1 is only effective at removing methyl groups from mono- or dimethylated H3K4 (Shi et al., 2004), it is capable of binding H3 peptides with trimethylated K4 residues (Stavropoulos et al., 2006), and knockdown of LSD1 has previously also been shown to increase levels of H3K4 trimethylation at target genes (Adamo et al., 2011). As such, whereas LSD1 may not be directly affecting the

trimethylated form of H3K4 under normal conditions, it is possible that its removal may provide a more optimum environment for histone methylation. The long intergenic RNA (lincRNA) *HOTAIR* has previously been shown to act as a modular scaffold by binding to and recruiting LSD1 to its chromatin targets and thus silencing gene expression (Tsai et al., 2010). Our data suggest that the *APOA1-AS* transcript identified here induces epigenetic regulation of *APOA1* in a similar manner, by mediating LSD1 occupancy across this locus. Treatment with our *APOA1-AS* siRNAs led to the disruption of this interaction, which coincided with an increase in H3K4 trimethylation within the region encompassing *APOA1* (P1–P4), thus resulting in enhanced gene expression. This would appear to be H3K4 specific because the *APOA1-AS* siRNA was not seen to affect the trimethylation state of H3K9, which is in line with previous reports that LSD1 demonstrates an extremely high affinity for H3K4 over H3K9 (Shi et al., 2004).

Similarly, various other lncRNAs have also recently been reported to physically interact with the PRC2 component SUZ12. For example, the NAT *ANRIL* mediates the silencing of tumor suppressor gene $p15^{INK4B}$ through physical recruitment of SUZ12, which in turn induces repressive H3K27 trimethylation (Kotake et al., 2011). Indeed, in addition to binding LSD1, *HOTAIR* has also been shown to repress the transcription of the human HOXD locus through its direct interaction with SUZ12 and, thus, the PRC2 complex (Tsai et al., 2010). Here, we demonstrate that knockdown of *APOA1-AS* leads to disruption of SUZ12 binding across the majority of the *APO* gene cluster and coincides with a reduction of H3K27 trimethylation marks along the promoter regions of *APOA1*, *APOA4*, and *APOC3*. Although this is likely to also promote *APOA1* gene expression, along with decreases in LSD1, a reduced occupancy of SUZ12 would also explain the observed increase in *APOA4* and *APOC3* expression in liver cells following *APOA1-AS* siRNA treatment.

Interestingly, no *trans* effect was indicated for the *APOA1-AS* on *APOA5*, which is located 28 kb downstream of the other three affected genes, nor was there any effect on the neighboring upstream gene *QSK*, which may indicate a boundary for the NAT's regulatory effect on the chromatin or the presence of insulator elements (Kim et al., 2007). Indeed, a previous study has shown that *APOA1/APOC3/APOA4* genes are organized into complex chromatin loops (Mishiro et al., 2009).

The locus-specific recruitment of histone-modifying complexes by NATs, observed here and in our other published report (Modarresi et al., 2012), suggests that approaches to modify these antisense transcripts may offer more control over target sense gene upregulation than compounds, such as LSD1 or PRC2 inhibitors, which could have a number of off-target effects. It should be noted that the use of ASOs to mediate RNA silencing can also be associated with off-target activity; however, the fact that the same effect of *APOA1* upregulation was observed following treatment with both siRNAs and modified AntagoNATs supports the specificity of the mechanism proposed here. Furthermore, the upregulation of *APOA1* observed during AntagoNAT screening and in vivo testing is unlikely attributed to general toxicity, as indicated by MTS toxicity assays, nor could it be an artifact of PS/2OMe/LNA/DNA chemistry load because much higher concentrations of the relevant control AntagoNATs were seen to have no effects. The present data show the effectiveness of a relatively low dose of CUR-962 in increasing *APOA1* mRNA and protein concentration in vivo in a primate model and highlight the potential applicability of AntagoNAT strategies for inducing therapeutic gene upregulation in a clinical setting. Although still in its infancy, further optimizing this approach could have advantages over current drug-based or viral gene therapy approaches due to the high specificity, stability, and potency of ASOs.

EXPERIMENTAL PROCEDURES

Cell Culture

All cell lines were maintained at 37°C and 5% CO_2 and passaged every 3–4 days. FBS from Mediatech (catalog #MT35-011-CV) was used in all cases. 518A2 and Vero76 cells were grown in DMEM plus 5% FBS. HepG2 cells were grown in EMEM (ATCC, catalog #2003) plus 10% FBS. African green monkey primary hepatocytes were grown in DMEM and isolated as previously reported by LeCluyse et al. (2005). All media contained penicillin/streptomycin (Mediatech, catalog #MT30-002-CI).

RACE

RACE was conducted using the firstChoice RLM-RACE Kit (Life Technologies, catalog #AM1700) as described by the manufacturer, followed by two successive nested PCRs of the cDNA copies. The PCR products were cloned and sequenced by Davis Sequencing.

Transient Transfections

For each transfection of active siRNA and negative control siRNA, 400 μl of OptiMEM was mixed gently with 4 μl of Lipofectamine 2000 (Invitrogen), and 20 ng of active/negative siRNA was added to the above mixture and incubated for 20 min at room temperature. After 20 min, 400 μl of OptiMEM plus Lipofectamine plus siRNA mixture was added to the HepG2 cells (2×10^5 cells/well) that were seeded into 6-well plates (35 mm) in EMEM plus 10% FBS. Cells were maintained at 37°C and 5% CO_2. After 24 hr, media were replaced with fresh EMEM plus 10% FBS. At 48 hr after transfection, cells were collected, and the RNA was extracted using QIAGEN RNA extraction column according to the manufacturer's protocol.

RNA Extraction

Total RNA was isolated using QIAGEN Midi RNA Extraction kit or SV Total RNA Isolation System from Promega (catalog #Z3105) following the manufacturers' instructions.

Reverse Transcription and qPCR

Reverse-transcription reaction was performed using the High-Capacity cDNA Kit from Applied Biosystems (catalog #4368813) as described in the manufacturer's protocol. Real-time PCR was conducted using ABI TaqMan Gene Expression Mix (catalog #4369510), and probes were designed by ABI (assay ID #Hs00202021_m1 for *APOA1*) on the StepOnePlus Real-Time PCR System (Applied Biosystems). The data were normalized to 18S expression (ABI; catalog #4319413E).

ChIP Assay

HepG2 cells were grown in EMEM (ATCC; catalog #2003) plus10% FBS and transiently transfected with 20 ng of control and *APOA1-AS* siRNAs according to the transient transfection protocol explained above. For H3K4me3, H3K9me3, and H3K27me3 experiments, at 48 hr after transfection, $\sim 2 \times 10^7$ cells were trypsinized, collected, and washed with ice-cold PBS three times, and the cell pellet was resuspended in cell lysis buffer (85 mM KCl, 0.5% Nonidet P-40, and 5 mM HEPES [pH 8.0]) supplemented with protease inhibitor cocktail (Roche), incubated on ice for 15 min, and centrifuged at 3,500 × *g* for 5 min to pellet the nuclei. The pellet was resuspended in nuclear lysis buffer (50 mM HEPES-KOH [pH 7.5], 140 mM NaCl, 1 mM EDTA [pH 8.0], 1% Triton X-100, 0.1% sodium deoxycholate, and 0.1% SDS) at a ratio of 2:1

(v/v) relative to the initial cell pellet volume and incubated on ice for 10 min. The solution was sonicated to obtain chromatin fragments of 100–1,000 bp using bioruptor for 10 min with 30 s on and 30 s off cycles. The sonicated lysate was centrifuged at 13,000 rpm for 5 min at 4°C, and the supernatant was aliquoted for each ChIP reaction including one aliquot as input.

Each aliquot was diluted to ten times with RIPA buffer (50 mM Tris-HCl [pH 8.0], 150 mM NaCl, 2 mM EDTA [pH 8.0], 1% NP-40, 0.5% sodium deoxycholate, and 0.1% SDS) supplemented with protease inhibitor cocktail (Roche) and PMSF. Five micrograms of antibody, including IgG as a control, was added to each ChIP and incubated at 4°C for 4 hr with rotation. Twenty microliters of protein A/G bead mixture (preadsorbed with sonicated single-stranded herring sperm DNA and BSA for 30 min at room temperature) was added to all samples and immunoprecipitated for 2 hr at 4°C with rotation.

The beads were collected using a magnetic rack (Invitrogen), and the supernatant was discarded. The beads were washed with 1 ml of the buffer in the following order: 3× with low-salt buffer (0.1% SDS, 1% Triton X-100, 2 mM EDTA [pH 8.0], 150 mM NaCl, and 20 mM Tris-HCl [pH 8.0]), 1× with high-salt buffer (0.1% SDS, 1% Triton X-100, 2 mM EDTA [pH 8.0], 500 mM NaCl, and 20 mM Tris-HCl [pH 8.0]), and 2× with TE buffer, each time washing the beads with rotation for 5 min at 4°C and discarding the supernatant. The beads were then incubated with 200 μl of DNA elution buffer (1% SDS and 100 mM NaHCO3) at room temperature, and the supernatant was collected. DNA was purified from the eluate using QIAGEN DNA Mini Kit following the manufacturer's protocol.

For SUZ12 and LSD1 experiments, prior to cell lysis, the transfected cells were collected and crosslinked by adding 1% formaldehyde for 10 min at room temperature. The reaction was quenched by adding 125 mM glycine for 5 min at room temperature. Washing, lysis, resuspension, sonication, and immunoprecipitation aliquoting were performed as above. A total of 8 μg of antibody, including IgG as a control, was incubated with 50 ml Dynabeads Protein G (Life Technologies) for 30 min at room temperature. This antibody/Dynabeads mixture was added to all samples and incubated overnight at 4°C with rotation. The beads were collected and washed as above. To reverse the crosslinking and elute DNA, the beads/antibody/antigen complexes were suspended in elution buffer (1% SDS, 100 mM $NcHCO_3$, 200 mM NaCl, 50 mM Tris-HCL [pH 8.0], 10 mM EDTA [pH 8.0], and 2.5% proteinase K) at 65°C for 4 hr, with shaking. Purification of DNA from the eluates was performed as above.

APOA1 ELISA Analysis

ELISA plates were coated overnight with mAb HDL110 (Mabtech APOA1 ELISA kit, catalog # 3710-11-6, 1,000 μg/ml) diluted 1:500 in Coating buffer (Immunochemistry Technologies; catalog #644), washed with TBST, and blocked with Blocker BSA (Pierce; catalog #37520)/0.5% Tween 20 for 30 min at room temperature. APOA1 standard from the Mabtech APOA1 ELISA kit was used to generate standard curve. Samples were loaded on a plate and incubated for 2 hr at room temperature, then washed and incubated with detection antibody (mAb HDL44biotin) from the kit diluted in block (1:2,000), washed and incubated with streptavidin from the kit in block (1:1,000) for 1 hr at room temperature, and washed again. Then substrate (LabVision, TMB Fisher, catalog # TA060TMB) was added and incubated for 10–20 min at room temperature. Plates were read at 650 nm.

Primate Studies

In vivo studies were conducted at the St. Kitts Biomedical Research Foundation, in full compliance with the NIH Guide for the Care and Use of Animals. Baseline clinical exams, including clinical chemistries, were conducted on eight adult female African green monkeys to confirm good health and suitability for study enrollment. Monkeys were fed approximately 120 g standard monkey chow (Teklad) per day. The monkeys were assigned to two treatment groups of four animals each and dosed once daily between 7:00 and 10:00 a.m. on study days 1, 3, and 5 by intravenous saphenous vein infusion over ~15–20 min at a rate of 24 ml/kg/hr. The animals were sedated with ketamine and xylazine intramuscularly (5.0 mg/kg ketamine/1.0 mg/kg xylazine) prior to and during the dosing procedure. Blood samples were obtained via superficial venipuncture from all animals at three baseline time points prior to treatment. Additional blood samples were collected at intervals postdosing, and plasma APOA1 protein concentrations were assessed by immunoturbidimetric assay. The animals did not have access to food for 12 hr prior to collecting all samples, in order to ensure that any observed changes in APOA1 measurements were not due to dietary reasons. They were then fed again immediately after the samples were taken. A percutaneous liver biopsy was performed on all study monkeys, under ketamine and xylazine sedation, at the first baseline sampling time point and on study day 7. An INRAD 14G biopsy needle was employed to obtain four core biopsies (~1.5 cm in length) from the right lobe of the liver. Biopsies were immediately immersed in a labeled cryotube containing 2 ml of RNAlater (QIAGEN) and incubated at 4°C overnight, following which the RNAlater was aspirated and the sample tube flash frozen in liquid nitrogen for transportation prior to total RNA isolation for real-time qPCR.

SUPPLEMENTAL INFORMATION

Supplemental Information includes six figures and one table and can be found with this article online at http://dx.doi.org/10.1016/j.celrep.2013.12.015.

Received: August 20, 2012
Revised: April 3, 2013
Accepted: December 10, 2013
Published: January 2, 2014

REFERENCES

Adamo, A., Sesé, B., Boue, S., Castaño, J., Paramonov, I., Barrero, M.J., and Izpisua Belmonte, J.C. (2011). LSD1 regulates the balance between self-renewal and differentiation in human embryonic stem cells. Nat. Cell Biol. *13*, 652–659.

Ansari, A.Z. (2009). Riboactivators: transcription activation by noncoding RNA. Crit. Rev. Biochem. Mol. Biol. *44*, 50–61.

Antonarakis, S.E., Oettgen, P., Chakravarti, A., Halloran, S.L., Hudson, R.R., Feisee, L., and Karathanasis, S.K. (1988). DNA polymorphism haplotypes of the human apolipoprotein APOA1-APOC3-APOA4 gene cluster. Hum. Genet. *80*, 265–273.

Barbaras, R., Puchois, P., Fruchart, J.C., and Ailhaud, G. (1987). Cholesterol efflux from cultured adipose cells is mediated by LpAI particles but not by LpAI:AII particles. Biochem. Biophys. Res. Commun. *142*, 63–69.

Calin, G.A., and Croce, C.M. (2006). MicroRNA signatures in human cancers. Nat. Rev. Cancer *6*, 857–866.

Camblong, J., Iglesias, N., Fickentscher, C., Dieppois, G., and Stutz, F. (2007). Antisense RNA stabilization induces transcriptional gene silencing via histone deacetylation in S. cerevisiae. Cell *131*, 706–717.

Cao, R., Wang, L., Wang, H., Xia, L., Erdjument-Bromage, H., Tempst, P., Jones, R.S., and Zhang, Y. (2002). Role of histone H3 lysine 27 methylation in Polycomb-group silencing. Science *298*, 1039–1043.

Dias, N., and Stein, C.A. (2002). Antisense oligonucleotides: basic concepts and mechanisms. Mol. Cancer Ther. *1*, 347–355.

Eisenberg, S. (1984). High density lipoprotein metabolism. J. Lipid Res. *25*, 1017–1058.

Elshourbagy, N.A., Boguski, M.S., Liao, W.S., Jefferson, L.S., Gordon, J.I., and Taylor, J.M. (1985). Expression of rat apolipoprotein A-IV and A-I genes: mRNA induction during development and in response to glucocorticoids and insulin. Proc. Natl. Acad. Sci. USA *82*, 8242–8246.

Faghihi, M.A., and Wahlestedt, C. (2009). Regulatory roles of natural antisense transcripts. Nat. Rev. Mol. Cell Biol. *10*, 637–643.

Faghihi, M.A., Kocerha, J., Modarresi, F., Engström, P.G., Chalk, A.M., Brothers, S.P., Koesema, E., St Laurent, G., and Wahlestedt, C. (2010). RNAi screen indicates widespread biological function for human natural antisense transcripts. PLoS ONE *5*, e13177.

Glomset, J.A. (1968). The plasma lecithins:cholesterol acyltransferase reaction. J. Lipid Res. *9*, 155–167.

Green, P.H., Glickman, R.M., Saudek, C.D., Blum, C.B., and Tall, A.R. (1979). Human intestinal lipoproteins. Studies in chyluric subjects. J. Clin. Invest. *64*, 233–242.

Guttman, M., Donaghey, J., Carey, B.W., Garber, M., Grenier, J.K., Munson, G., Young, G., Lucas, A.B., Ach, R., Bruhn, L., et al. (2011). lincRNAs act in the circuitry controlling pluripotency and differentiation. Nature *477*, 295–300.

Huarte, M., Guttman, M., Feldser, D., Garber, M., Koziol, M.J., Kenzelmann-Broz, D., Khalil, A.M., Zuk, O., Amit, I., Rabani, M., et al. (2010). A large intergenic noncoding RNA induced by p53 mediates global gene repression in the p53 response. Cell *142*, 409–419.

Kaikkonen, M.U., Lam, M.T.Y., and Glass, C.K. (2011). Non-coding RNAs as regulators of gene expression and epigenetics. Cardiovasc. Res. *90*, 430–440.

Katayama, S., Tomaru, Y., Kasukawa, T., Waki, K., Nakanishi, M., Nakamura, M., Nishida, H., Yap, C.C., Suzuki, M., Kawai, J., et al.; RIKEN Genome Exploration Research Group; Genome Science Group (Genome Network Project Core Group); FANTOM Consortium (2005). Antisense transcription in the mammalian transcriptome. Science *309*, 1564–1566.

Kim, T.H., Abdullaev, Z.K., Smith, A.D., Ching, K.A., Loukinov, D.I., Green, R.D., Zhang, M.Q., Lobanenkov, V.V., and Ren, B. (2007). Analysis of the vertebrate insulator protein CTCF-binding sites in the human genome. Cell *128*, 1231–1245.

Kotake, Y., Nakagawa, T., Kitagawa, K., Suzuki, S., Liu, N., Kitagawa, M., and Xiong, Y. (2011). Long non-coding RNA ANRIL is required for the PRC2 recruitment to and silencing of p15(INK4B) tumor suppressor gene. Oncogene *30*, 1956–1962.

Kouzarides, T. (2002). Histone methylation in transcriptional control. Curr. Opin. Genet. Dev. *12*, 198–209.

Kuzmichev, A., Nishioka, K., Erdjument-Bromage, H., Tempst, P., and Reinberg, D. (2002). Histone methyltransferase activity associated with a human multiprotein complex containing the Enhancer of Zeste protein. Genes Dev. *16*, 2893–2905.

LeCluyse, E.L., Alexandre, E., Hamilton, G.A., Viollon-Abadie, C., Coon, D.J., Jolley, S., and Richert, L. (2005). Isolation and culture of primary human hepatocytes. Methods Mol. Biol. *290*, 207–229.

Lehner, B., Williams, G., Campbell, R.D., and Sanderson, C.M. (2002). Antisense transcripts in the human genome. Trends Genet. *18*, 63–65.

Livshits, G., Vainder, M., Graff, E., Blettner, M., Schettler, G., and Brunner, D. (1997). Tel-Aviv-Heidelberg Three Generation Offspring Study: genetic and environmental sources of variation and covariation among plasma lipids, lipoproteins, and apoliproteins. Am. J. Hum. Biol. *9*, 357–370.

Magistri, M., Faghihi, M.A., St Laurent, G., 3rd, and Wahlestedt, C. (2012). Regulation of chromatin structure by long noncoding RNAs: focus on natural antisense transcripts. Trends Genet. *28*, 389–396.

Martinho, R.G., Kunwar, P.S., Casanova, J., and Lehmann, R. (2004). A noncoding RNA is required for the repression of RNApolII-dependent transcription in primordial germ cells. Curr. Biol. *14*, 159–165.

McDermott, A.M., Heneghan, H.M., Miller, N., and Kerin, M.J. (2011). The therapeutic potential of microRNAs: disease modulators and drug targets. Pharm. Res. *28*, 3016–3029.

Miller, B.H., and Wahlestedt, C. (2010). MicroRNA dysregulation in psychiatric disease. Brain Res. *1338*, 89–99.

Mishiro, T., Ishihara, K., Hino, S., Tsutsumi, S., Aburatani, H., Shirahige, K., Kinoshita, Y., and Nakao, M. (2009). Architectural roles of multiple chromatin insulators at the human apolipoprotein gene cluster. EMBO J. *28*, 1234–1245.

Modarresi, F., Faghihi, M.A., Lopez-Toledano, M.A., Fatemi, R.P., Magistri, M., Brothers, S.P., van der Brug, M.P., and Wahlestedt, C. (2012). Inhibition of natural antisense transcripts in vivo results in gene-specific transcriptional upregulation. Nat. Biotechnol. *30*, 453–459.

Nagano, T., Mitchell, J.A., Sanz, L.A., Pauler, F.M., Ferguson-Smith, A.C., Feil, R., and Fraser, P. (2008). The Air noncoding RNA epigenetically silences transcription by targeting G9a to chromatin. Science *322*, 1717–1720.

Pastori, C., and Wahlestedt, C. (2012). Involvement of long noncoding RNAs in diseases affecting the central nervous system. RNA Biol. *9*, 860–870.

Rader, D.J. (2002). High-density lipoproteins and atherosclerosis. Am. J. Cardiol. *90* (8A), 62i–70i.

Rinn, J.L., Kertesz, M., Wang, J.K., Squazzo, S.L., Xu, X., Brugmann, S.A., Goodnough, L.H., Helms, J.A., Farnham, P.J., Segal, E., and Chang, H.Y. (2007). Functional demarcation of active and silent chromatin domains in human HOX loci by noncoding RNAs. Cell *129*, 1311–1323.

Shi, Y., Lan, F., Matson, C., Mulligan, P., Whetstine, J.R., Cole, P.A., Casero, R.A., and Shi, Y. (2004). Histone demethylation mediated by the nuclear amine oxidase homolog LSD1. Cell *119*, 941–953.

Sleutels, F., Zwart, R., and Barlow, D.P. (2002). The non-coding Air RNA is required for silencing autosomal imprinted genes. Nature *415*, 810–813.

Stavropoulos, P., Blobel, G., and Hoelz, A. (2006). Crystal structure and mechanism of human lysine-specific demethylase-1. Nat. Struct. Mol. Biol. *13*, 626–632.

Strahl, B.D., and Allis, C.D. (2000). The language of covalent histone modifications. Nature *403*, 41–45.

Taft, R.J., Pang, K.C., Mercer, T.R., Dinger, M., and Mattick, J.S. (2010). Non-coding RNAs: regulators of disease. J. Pathol. *220*, 126–139.

Tsai, M.C., Manor, O., Wan, Y., Mosammaparast, N., Wang, J.K., Lan, F., Shi, Y., Segal, E., and Chang, H.Y. (2010). Long noncoding RNA as modular scaffold of histone modification complexes. Science *329*, 689–693.

van Rooij, E., and Olson, E.N. (2007). MicroRNAs: powerful new regulators of heart disease and provocative therapeutic targets. J. Clin. Invest. *117*, 2369–2376.

Veedu, R.N., and Wengel, J. (2009). Locked nucleic acid as a novel class of therapeutic agents. RNA Biol. *6*, 321–323.

Wahlestedt, C. (2006). Natural antisense and noncoding RNA transcripts as potential drug targets. Drug Discov. Today *11*, 503–508.

Wang, J., Lu, F., Ren, Q., Sun, H., Xu, Z., Lan, R., Liu, Y., Ward, D., Quan, J., Ye, T., and Zhang, H. (2011a). Novel histone demethylase LSD1 inhibitors selectively target cancer cells with pluripotent stem cell properties. Cancer Res. *71*, 7238–7249.

Wang, K.C., Yang, Y.W., Liu, B., Sanyal, A., Corces-Zimmerman, R., Chen, Y., Lajoie, B.R., Protacio, A., Flynn, R.A., Gupta, R.A., et al. (2011b). A long noncoding RNA maintains active chromatin to coordinate homeotic gene expression. Nature *472*, 120–124.

Zamore, P.D., Tuschl, T., Sharp, P.A., and Bartel, D.P. (2000). RNAi: double-stranded RNA directs the ATP-dependent cleavage of mRNA at 21 to 23 nucleotide intervals. Cell *101*, 25–33.